Z. Phys. D 35, 141–148 (1995)

ZEITSCHRIFT
FÜR PHYSIK D

Microscopic structure of collective density oscillations C_{60} and C_{70}

M.S. Hansen[1,†], **J.M. Pacheco**[2], **G. Onida**[3]

[1] The Niels Bohr Institute, University of Copenhagen, DK-2100 Copenhagen Ø, Denmark
[2] Departamento de Fisica da Universidade, P-3000 Coimbra, Portugal
[3] Laboratoire des Solides Irradiés, URA CNRS 1380-CEA/DTA/DECM, Ecole Polytechnique, F-91128 Palaiseau, France

Received: 27 May 1995

Abstract. The microscopic structure of the photo-excited plasmon excitation in C_{60} and C_{70} is investigated using linear response theory. One finds that Landau damping provides the main contribution to the lineshape and the linewidth of the Mie-type plasmon being able, in the case of C_{70}, to mask the deformation splitting effect associated with the low equilibrium symmetry (D_{5h}) of this fullerene. Furthermore, it is found that the coupling of the plasmon to the normal modes of vibration of the fullerenes provides a sizeable contribution to the lineshape, without significantly affecting the linewidth. This coupling is found to be active already at $T = 0$, exhibiting a weak temperature dependence.

PACS: 36.40.+d; 31.50.+w; 33.20.Kf

1 Introduction

1.1 C_{60}

Stimulated by measurements of the photoabsorption strength in the C_{60} fullerene [1], Bertsch et al. [2] have calculated its electromagnetic response. The calculation has been carried out making use of linear response theory within the one-electron basis provided by the tight-binding approximation. Theory has been quite successful in reproducing the available experimental data and in predicting a Mie-type resonance at ≈ 20 eV which has been observed in later experiments performed on gas-phase C_{60} [3]. Extensions of this original tight-bindfing calculation have been developed and the multipole plasmon excitations in fullerenes have been computed [4] and measured [5,6]. More recently, a *state of the art* calculation of the photoresponse of C_{60} has been carried out in [7], incorporating the full icosahedral symmetry of the fullerene, and describing the ionic cores via norm-conserving, non-local pseudopotentials. The valence electrons of all carbon atoms were treated in the Local Density Approximation (LDA) to Density Functional Theory (DFT), and the optical absorption calculated making use of linear response theory in the so-called Time-Dependent LDA (TDLDA). In Fig. 1 we put together the theoretical results mentioned before for the optical response in comparison with the experimental data of [3]: the tight-binding linear response (TB-LR) results of [2] are drawn with a full curve, the TDLDA results [7] are displayed with a dotted line and the experimental data [3] are drawn with black dots.

The experimental method utilized in [3] provides relative values for the cross section, probing the photoresponse only at excitation energies above the ionization threshold. Therefore, it provides no direct information on the amount of strength measured. Consequently, a direct comparison of the three curves requires a rescaling which is now described. Concerning the theoretical methods, the TDLDA results shown ($E \leq 35$ eV) exhaust about 85% of the Thomas-Reiche-Kuhn (TRK) sum-rule, which establishes a theoretical upper bound to the total oscillator strength. As for the TB-LR model, the small size of the one-electron basis used in the computation of the optical response (Fig. 2), together with the non-local nature of the tight-binding hamiltonian, lead to strong deviations from the TRK sum-rule value. As a result, the TB-LR exhausts only 35% of the TRK sum-rule value of 240, the number of active (valence) electrons in the molecule. In view of this, the results shown in Fig. 1 have been scaled in the following way: the TDLDA results are taken as the reference curve; the experimental results are then rescaled in order to maximize the overlap with the TDLDA results. Then, the TB-LR results have been rescaled in such a way that the sum-rule exhausted in the energy window probed experimentally is the same as the experimental value. Both theoretical curves have been folded with Lorentzian functions characterized by an intrinsic width $\Gamma = 0.06E$.

The TDLDA curve in Fig. 1 provides an overall account of the experimental data [8]. Also, the TB-LR

† We would like to dedicate this work to Michael Hansen, who actively participated in most of the work and studies carried out in this paper, and who is not among us anymore

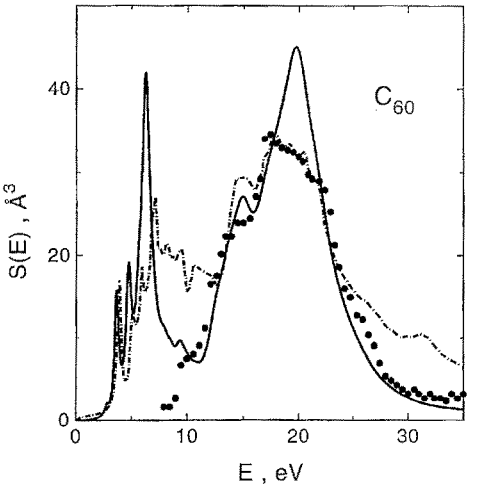

Fig. 1. Photoabsorption strength of C_{60} obtained by different methods: the experimental data of [3] are drawn with *black dots*. The tight binding results are drawn with a *full curve*, whereas the ab initio results of [7] are drawn with a *dotted curve* (for details, see main text)

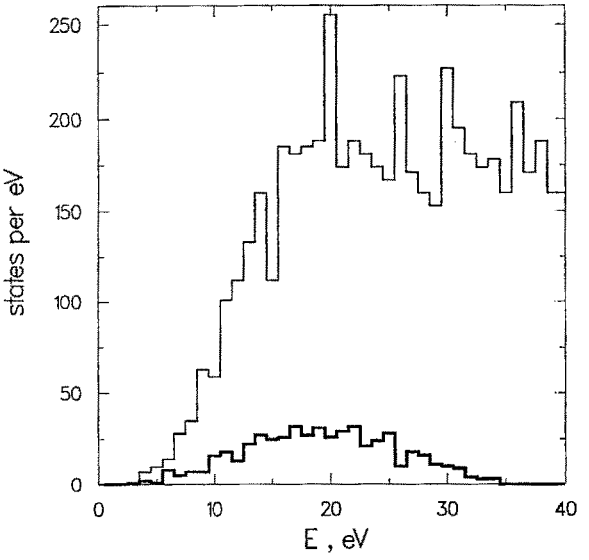

Fig. 2. Number of one-electron dipole transitions per eV, for C_{60}. The *thick curve* displays the tight-binding results, whereas the *thin curve* shows the corresponding quantity as obtained in [7]. Clearly, there is a dramatic difference in both methods, which qualitatively explains why the TB-LR does not account for the rather flat top of the Mie-type plasmon, which is observed experimentally and very well reproduced by the TDLDA calculation (Fig. 1)

formulation is able to account for the mean energy position of the plasmon (on the foregoing, we shall call plasmon to the photo-excited collective density oscillations in the fullerenes) excitation, both in the so-called π-plasmon region (≈ 6 eV) and the σ-plasmon region (≈ 20 eV). This puts into evidence the role played by Landau damping in the lineshape and linewidth of the plasmon in C_{60}, since it is the only relaxation mechanism operative in linear response theory, at the energy of the Mie-type plasmon. We would like to point out that both calculations take into account the full icosahedral symmetry of the molecule as well as the screening of the electron–electron interaction, features which were found essential for an appropriate description of the optical response of C_{60} [7]. This, together with a computational cost that is many orders of magnitude lower than the ab initio calculation of [7], make the TB-LR formulation appropriate for the study to be carried out below.

In order to have a detailed understanding of the lineshape and linewidth of the plasmon, one needs to investigate the role played, not only by Landau damping, but also by other relaxation mechanisms. The coupling of a collective mode (such as the plasmon) to the normal modes of vibration of the ions, the coupling to large amplitude surface fluctuations, or the coupling to more complicated many-electron configurations with a nearly degenerate excitation energy, are known to play a role in general many-electron [9] and many-fermion [10, 11] systems, both at zero [10, 12] and at finite [9, 11] temperature. To study them, one needs to go beyond linear response. Furthermore, and in what concerns the linewidth, it is well known that the contribution to the total width is not obtained by a simple sum of the widths associated with the different mechanisms contributing to it [9, 10, 13]. As a matter of fact, the theoretical curves in Fig. 1 already take these considerations into account, since the linewidth obtained can be interpreted as resulting from (at least) two different relaxation processes: (*i*) Landau damping and (*ii*) the one(s) responsible for the intrinsic width Γ which, instead of being simply added, is introduced in the formulation replacing the infinitesimal η in (4) (see Sect. 2). This energy-dependent Γ, the net result of which is to considerably smooth the lineshape (Fig. 4), is usually associated with (and has been obtained in) the coupling of the plasmon to the surface fluctuations of clusters [9]. Whether the parametrization used in [7] (and reproduced in Fig. 1) is adequate to C_{60} remains an open problem.

In this paper, we investigate the coupling of the plasmon, in C_{60} and C_{70}, to the normal modes of vibration of these fullerenes. Because an ab initio study of this coupling, along the lines of [7], is not feasible with present-day computer resources, and taking into account the performance of the TB-LR [2], we shall adopt this formulation in order to compute the optical response of C_{60} and C_{70} at different configurations (Sect. 2).

1.2 C_{70}

In [3], the plasmon excitation in gas-phase C_{70} has been detected as well. Its lineshape was found to be similar and somewhat smoother than the one of C_{60}, with essentially the same centroid energy and linewidth. This result has been rationalized in [3] by recognizing that the mean electronic densities of C_{60} and C_{70} are similar, thereby leading to the same mean energy for the plasmon excitation (plasmon-pole approximation). Besides the wealth of quantal effects which, being present in C_{60}, are also expected to play an important role in C_{70}, there is, already at the level of the plasmon-pole approximation, a geometric effect associated with the equilibrium shape of C_{70} which acts to produce a splitting of the Mie-type plasmon

resonance peak into two peaks, contrary to the single-peak structure associated with C_{60}. Indeed, C_{60} displays an isotropic behaviour with respect to an external dipole perturbation, in this respect behaving like a spherical object. This is a well-known feature directly related to its icosahedral equilibrium geometry, with 3 equivalent principal axes – Fig. 3a. On the other hand, C_{70} displays a different behaviour in the presence of a dipole external field, since its geometry embodies 2 equivalent principal axes (X and Y in Fig. 3b), and a third, more elongated one (Z-axis in Fig. 3b). The dipole oscillations will then take place at a lower frequency when along the Z-axis, as compared to oscillations in the X-Y-plane. This phenomenon will induce what is known in nuclear physics as "deformation splitting", a phenomenon also observed in microclusters [9]. Within the plasmon-pole approximation, one can in fact estimate this splitting to be of the order of 1 eV. However, to the extent that Landau damping is as prominent in C_{70} as in C_{60}, it is likely that this effect is not observable [14], leading to a lineshape and linewidth for C_{70} similar to the one for C_{60}. This is to be expected since, on general grounds, the density of one-electron excitations in the neighbourhood of the plasmon is larger for C_{70} than for C_{60}. Therefore, we start by calculating the optical response of C_{60} and C_{70}, making use of linear response theory. In agreement with the experimental results of [3], it will be found that both lineshapes associated with the Mie-type plasmon are similar. We then proceed to study the coupling of the plasmon to the normal modes of vibration of both fullerenes. To this end, we carry out this coupling beyond the linear response formulation, in the way developed below. It will be found that this coupling provides a sizeable smoothing contribution to the overall lineshape of the plasmon in C_{60} and C_{70}, irrespective of their vibrational temperature. In fact, alteady at $T = 0$, pure quantal zero-point fluctuations of the constituent carbon atoms are able to produce the smoothing effect, which is only weakly enhanced as the vibrational temperature is increased.

Our paper is organized as follows: In Sect. 2 we start by summarizing the linear response formulation we use, proceeding then to incorporate it in the coupling scheme which is also developed there. In Sect. 3 we discuss the main results obtained, their consequences, main conclusions and future prospects being collected in Sect. 4.

2 Theory

We shall adopt the same TB-LR formulation of [2]. The one-electron states are provided by the nearest-neighbour distance-dependent tight-biding hamiltonian,

$$H(\{\mathbf{R}_i\}) = \sum_{\alpha,i} \varepsilon_\alpha a^+_{\alpha,i} a_{\alpha,i} + \sum_{\alpha,\beta,i,j} t_{\alpha,i,\beta,j}(\{\mathbf{R}_i\}) a^+_{\alpha,i} a_{\beta,j}, \quad (1)$$

where latin indices label atomic sites and Greek indices label the different (s, p_x, p_y, p_z) atomic orbitals of each carbon atom. The quantities ε_α are the atomic-orbital energies and $t_{\alpha,i,\beta,j}(\{\mathbf{R}_i\})$ are the hopping matrix-elements between different sites, which have been fixed in order to produce a best fit to ab initio LDA ground-state calculations of carbon clusters (for details, [2] and references therein). The set of coordinates $(\{\mathbf{R}_i\})$ specifies the position of all carbon atoms in a molecule-fixed reference frame, the different hopping matrix-elements depending parametrically on these coordinates. In keeping with the formulation of [2], the collective plasmon excitations are calculated making use of linear response theory, in which the screening of the external field is incorporated approximately via a separavble dipole–dipole interaction, where the dipole operator is written,

$$D_z = D_Z^{(1)} + D_Z^{(2)} = e \sum_{\alpha,i} z_i(\{\mathbf{R}_i\}) a^+_{\alpha,i} a_{\alpha,i} + ed \sum_i (a^+_{s,i} a_{p_z,i} + a^+_{p_z,i} a_{s,i}), \quad (2)$$

that is, the sum of the overall dipole moment of the charge distribution and the dipole moment on each site. In (2), $z_i(\{\mathbf{R}_i\})$ is the z-coordinate of the i-th carbon atom, and d is the $s - p_z$ dipole matrix-element of a carbon atom. The screened dipole polarizability $\alpha(\omega)$ is then obtained, for each ω, by solving the 2×2 matrix equation (for details, cf. [2])

$$\tilde{\alpha} = [\tilde{1} + \widetilde{\alpha^{(0)}} \tilde{V})]^{-1} \widetilde{\alpha^{(0)}} \quad (3)$$

where $\widetilde{\alpha^0(\omega)}$ is the unscreened, independent particle polarizability of the system, with matrix-elements

$$\widetilde{\alpha^{(0)}}_{n,m}(\omega) = \sum_{p,h} \langle p | D_Z^{(n)} | h \rangle \langle h | D_Z^{(m)} | p \rangle \times \frac{2(\varepsilon_p - \varepsilon_h)}{(\varepsilon_p - \varepsilon_h)^2 - (\omega + i\eta)^2}. \quad (4)$$

The strength function $S(\omega)$ plotted, e.g., in Fig. 1, is directly related to the imaginary part of the polarizability:

$$S(\omega) = \frac{1}{\pi} Im[\alpha(\omega)]. \quad (5)$$

Once we have obtained an optical absorption profile which depends parametrically on the ionic coordinates, we are now in conditions to establish the adiabatic coupling of this excitation to the ionic vibrations of the fullerene. Indeed, both at zero and at finite temperature, the ions will vibrate around their equilibrium positions. In the Born-Oppenheimer approximation which is implicit in the present calculation, one assumes that the time-scale for the electrons is much shorter than the corresponding one for the ions, and therefore the coupling between the electronic response and the ionic motion can be carried out in the adiabatic approximation. Consequently, we include the effect of the ionic vibrations by statistically averaging over the possible configurations of the system. Denoting by $\hbar\omega_n$ the energy of the n-th normal mode and by $q_n(\{\mathbf{R}_i\})$ the associated normal displacement from equilibrium, the expression for the averaged strength function can be written,

$$\langle S(\omega) \rangle_T = \int dq_1 \cdots \int dq_n P(\{q_n\}, T) S(\{q_n\}, \omega). \quad (6)$$

The quantity $P(\{q_n\}, T)$ reads [15],

$$P(\{q_n\}, T) = \left[\prod_{n=1}^{N_{vib}} \left[\frac{\Omega_n}{\pi} \right]^{1/2} \right] \exp\left\{ -\sum_n \Omega_n q_n^2 \right\}, \quad (7)$$

where

$$\Omega_n = \frac{M_C \omega_n}{\hbar} \tanh\left[\frac{\hbar\omega_n}{2K_B T}\right], \tag{8}$$

M_C being the mass of a carbon ion, K_B the Boltzmann constant and T the fullerene internal vibrational temperature [16]. The above expression is exact displaying the right low and high temperature limits. In fact, at zero temperature, this expression corresponds to averaging taking as a probability distribution the modulus squared of the harmonic oscillator ground-state product wavefunction associated with the different normal modes. It converges to the classical Boltzmann distribution at high T [15]. The calculation of the integrals is rather time consuming due to their large dimensionality. Still, it has been efficiently optimized by adopting a Monte-Carlo technique, in which importance sampling can be fully exploited [17, 18] taking into account the (in our case) separable gaussian probability density (7). It should be noted that, for Monte-Carlo integration to produce reliable results, several thousands of parametric response calculations have to be computed, this being usually the bottleneck of this type of calculations. Furthermore, in the quasi-random sampling of the mulidimensional space, the underlying group symmetry displayed by the molecule in its ground-state configuration is systematically broken, a feature which precludes the use of ab initio calculations whose efficiency is often optimized by exploiting particular group properties (symmetry adapted basis-sets, conserved quantum-numbers, etc.). In our case, because of the fast and efficient TB method utilized, all integrations were carried out in a DEC-300 workstation.

3 Results and discussion

We start by computing the optical response of C_{60} and C_{70} at their equilibrium positions, corresponding to the geometries displayed in Fig. 3. For C_{60} there are two different bond-lengths (r_i): r_p for the pentagonal "single"-bonds and r_h for the hexagonal "double"-bonds, whereas for C_{70} there are 8 different r_i. The values used are quoted in Table 1, and were taken from [19]. The results for the optical response of both fullerenes are displayed with thick solid lines in Figs. 4 and 5. The screened response function as obtained in [2] for C_{60} is displayed in Fig. 4, whereas Fig. 5 displays the screened response of C_{70}. Here we disentangle the contributions due to the dipole oscillations along the 2-inequivalent principal directions. The dotted line corresponds to the response along the z-axis (Fig. 3), which exhausts [14] 1/3 of the TRK sum-rule. The thin solid line corresponds to the response along the other two equivalent directions, and which exhausts 2/3 of the TRK sum-rule. The total response corresponds to the sum, and is displayed with a thick solid line. As already found in [2], the TB-LR formulation strongly violates the TRK sum-rule. We find a similar behaviour for both C_{60} and C_{70}, in which the TB-LR results exhausts about one third of the sum-rule. The results shown have been rescaled in order to exhaust 100% of the strength. A constant value of 0.2 eV was used for the imaginary part η (4), in order to obtain a smooth lineshape (this value will be used throughout this paper except where explicitly stated). The Full Width at Half Maximum (FWHM) is insensitive to this value, as long as

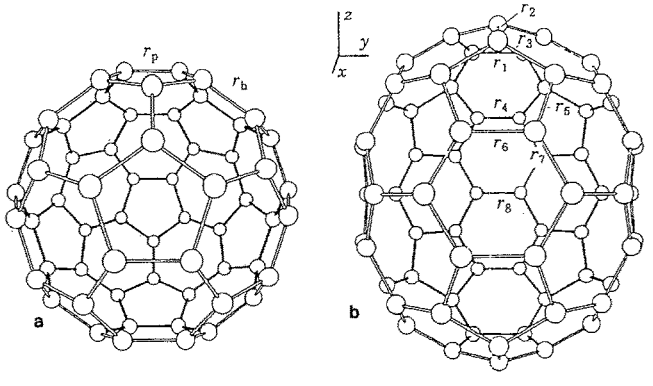

Fig. 3a, b. Equilibrium geometries utilized in this paper for the fullerenes C_{60} and C_{70}. The different r_i used and explicitly shown in the figure are given in Table 1

Table 1. Different bond-lengths (in Å) corresponding to the equilibrium geometries of C_{60} and C_{70} adopted in the present work, and explicitly shown in Fig. 3

C_{60}		C_{70}	
r_p	1.45	r_1	1.448
r_h	1.39	r_2	1.393
		r_3	1.444
		r_4	1.386
		r_5	1.442
		r_6	1.434
		r_7	1.415
		r_8	1.467

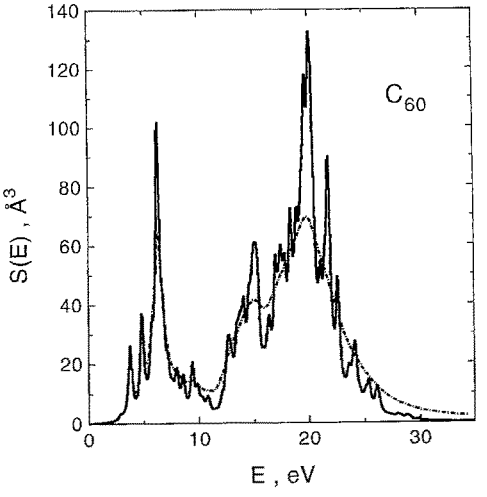

Fig. 4. Strength function $S(E)$ for C_{60} (*solid line*) as obtained for its equilibrium geometry making use of the Tight-Binding Linear Response. A constant value $\eta = 0.2$ eV (see main text for details) has been used in producing this curve. The *dotted line* shows the same curve obtained making $\eta = 0.06E$ (Fig. 1). The main effect of this different parametrization is to considerably smooth the resulting strength function, without significantly changing its linewidth

$\eta \ll$ FWHM [20]. As expected, the response along the two inequivalent directions is different, reflecting the spatial anisotropy of the C_{70} molecule. However, and irrespective of the small density of one electron excitations incorporated in the TB-LR model, Landau damping is the dominant feature underlying the optical response, totally masking the ≈ 1 eV deformation splitting effect discussed before. We would like to point out, however, that in order to have a detailed description of the lineshape of the plasmon in C_{70}, and for reasons similar to the ones already advanced for C_{60}, and which were put in evidence in Fig. 1, it is necessary to carry out a better linear response calculation, e.g., along the lines of [7]. This is presently being carried out [21]. We proceed now to study the effect of the ionic vibrations on the photoresponse of both fullerenes.

According to (6) and (7), in order to study the coupling we need the normal mode energies and the normal displacements from the equilibrium geometries. They were taken from the results of [19, 22]. The calculations in [19, 22] were carried out making use of the bond-charge model and, as discussed at length there, the results show a good agreement with the experimental data. There are 174 normal modes for C_{60}, and 204 modes for C_{70}. These are the dimensions of the multiple integrations in (6). We would like to point out that the vibrational spectrum of these two fullerenes is markedly different [19], being related to the very different equilibrium geometries displayed by C_{60} (Y_h) and C_{70} (D_{5h}), resulting in a highly degenerate spectrum for the former, whereas the larger fullerene displays somewhat softer and less degenerate modes.

For C_{60}, the lowest vibrational mode, a 5-fold degenerate H_g-mode, has an energy of ≈ 35 meV. It is noteworthy that a multipole decomposition of this mode reveals an almost pure quadrupole character. Furthermore, the lowest A_g mode, at an energy of ≈ 60 meV corresponds to the breathing mode of C_{60} (monopole character). Because of the dipolar character of the photon-induced plasmon excitations and the high symmetry associated with the icosahedral group to which C_{60} belongs, one might expect the ionic vibrations with a large monopole and quadrupole character to provide the most important decay channels, since they are the ones which couple directly to the photon field. Actually, in carrying out the integrals in (6) including only these modes, we find that their contribution is a small fraction of the overall effect obtained including all modes in an equal footing. The result of this full calculation is displayed in Fig. 6. The coupling was studied at three different temperatures, namely $T = 0$ K, $T = 300$ K, and a high-temperature limit of $T = 1200$ K. In Fig. 6 the thin solid line corresponds to the lineshape computed at the frozen equilibrium configuration (Fig. 4). The thick solid line was obtained by carrying out the coupling at $T = 0$, that is, including pure quantal zero-point fluctuations, and for which a sizeable effect is obtained. We would like to point out, however, that the net effect consists of a considerable smoothing of the lineshape, with no sizeable increase of the linewidth.

Indistinguishable from the $T = 0$ curve, is the lineshape obtained by establishing the coupling at $T = 300$ K. Finally, in the high temperature limit (1200 K), the dotted line was obtained, evidencing a further (though small) smoothing of the lineshape.

In all computations, 10000 configurations were sampled, with a probability density dictated by $P(\{q_n\}, T)$ (7). Of course, for a fixed amount of sampled points, the least accurate integral will correspond to C_{60} at $T = 1200$ K. Still, defining

$$A_{(n)} = \frac{1}{M} \sum_{q_i=1}^{M} \left[\sum_k [S(q_i, \omega_k) - S(q_i = 0, \omega_k)]^2 \right]^{(n)}, \qquad (9)$$

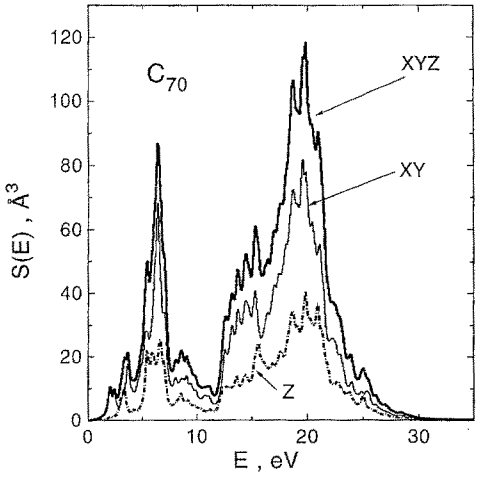

Fig. 5. Strength function for C_{70} obtained for its equilibrium configuration, using Tight-Binding Linear Response. Because of the anisotropy of C_{70}, the strength function is different, depending on whether the external field is oscillating along the Z-axis or along the X–Y plane (Fig. 3). The different contributions are explicitly indicated in the figure, whereas the total strength, obtained by summing the two curves, corresponds to the XYZ curve

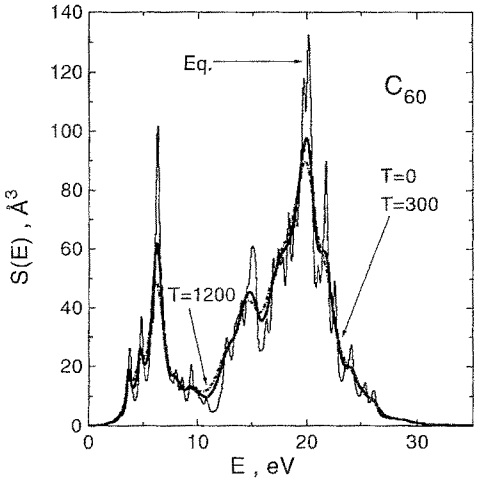

Fig. 6. Strength function of C_{60} obtained at different vibrational temperatures, as explicitly indicated. For reference, the lineshape obtained at equilibrium is also shown. The line $T = 0$, $T = 300$ corresponds, in fact, to two lineshapes obtained by carrying out the coupling at these two temperatures, and which cannot be distinguished by eye inspection

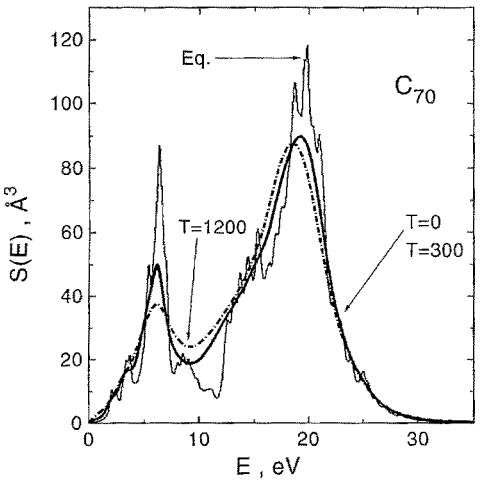

Fig. 7. Strength function of C_{70} obtained at different vibrational temperatures. Same notation as in Fig. 6

where M is the number of configurations sampled, the variance σ, given by [17]

$$\sigma = \left[\frac{\Lambda_{(2)} - \Lambda_{(1)}^2}{M-1} \right]^{(\frac{1}{2})}, \tag{10}$$

remains always below 0.02 for all cases studied here.

Figure 7 displays the corresponding results of integrating (6) for the 204 vibrational modes of C_{70}, at the same three temperatures used for C_{60} (also for C_{70}, 10000 sampled configurations have been used). As in Fig. 6, the thin solid line provides the reference equilibrium lineshape. The thick solid curve is obtained by coupling to zero-point fluctuations of the constituent atoms. The lineshape obtained for the coupling at $T = 300$ K cannot be distinguished, by eye-inspection, from the one at $T = 0$. For $T = 1200$ K (dotted line), a sizeable effect is also obtained, in which both lineshape and linewidth are affected. Comparing Figs. 6 and 7, we find a similar trend as a result of this coupling, which results in a sizeable effect, present already at $T = 0$, and which essentially contributes to smooth the otherwise more structured lineshape, without affecting the resulting linewidth. The coupling, in both fullerenes, exhibits a weak temperature dependence, C_{70} evidencing a larger broadening effect at high temperatures. We attribute the more sizeable temperature effect in C_{70} to its lower equilibrium symmetry (D_{5h}) as compared to C_{60} (Y_h). This lower symmetry not only leads to the anisotropic behaviour of the dipole response, as evidenced in Fig. 5, but also to a vibrational spectrum in which most of the degeneracies observed in C_{60} are removed [19].

On the other hand, only at high temperatures one observes deviations from the $T = 0$ coupling effect. In Fig. 8 we plot the energy of the normal modes (in ascending order) in C_{60} and C_{70}. The horizontal lines show the energy associated with the finite temperatures considered in the present study. One can observe that a temperature of 300 K is not enough to excite vibrational quanta in both fullerenes, whereas at $T = 1200$ K a sizeable fraction of the vibrational modes can be excited. This feature qualitatively explains why $T = 300$ K is no temperature

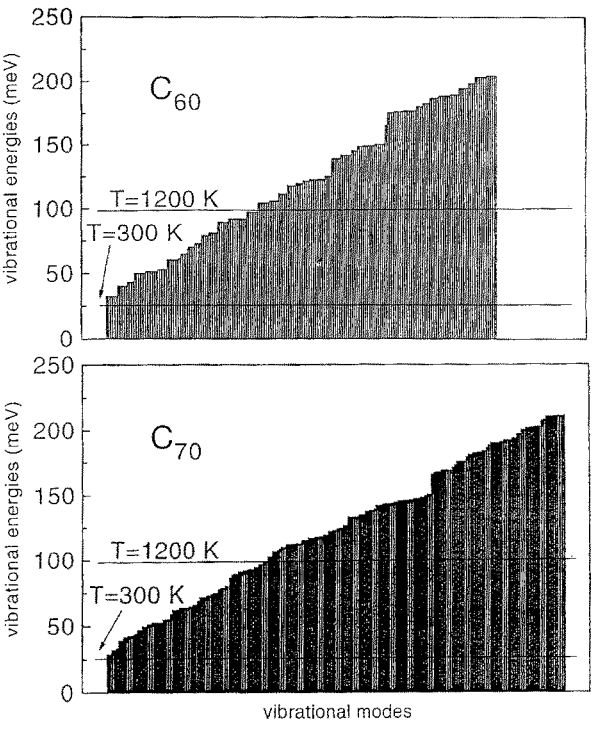

Fig. 8. The energies of the normal modes of C_{60} (*upper part*) and C_{70} (*lower part*), in meV, are plotted with vertical bars in ascending order. Since the plots use the same horizontal and vertical dimensions, the darker colour associated with the C_{70} part directly reflects the lower degeneracies present in its normal mode spectrum. As indicated, the *horizontal lines* give the energy scale for the finite temperature couplings considered in this work

for these clusters, and only at very high temperatures a thermal broadening can be expected. Furthermore, a detailed analysis of the contributions of the different modes to the total line broadening shows that no single symmetry is capable of producing the overall effect obtained, but instead one needs the full sampling of the multidimensional phase space to obtain the plotted results. Furthermore, many vibrational eigenmodes with high energy are associated with atomic displacements which are tangential with respect to the fullerene surface, inducing sizeable bond modulations, which provide the predominant contribution to the absorption lineshape. Indeed, such bond modulation effects have been recently predicted to occur in C_{60} [23] and C_{70} [24], due exclusively to the quantal zero-point motion of the atoms.

In [7], an intrinsic width $\eta = 0.06E$ has been used. In this way one takes into account, in a phenomenological way, all the other mechanisms which play a role in the lineshape and linewidth of the plasmon. In Fig. 9 we compare the C_{60} TB-LR lineshape, computed including the present coupling at $T = 300$ K (solid line), and the corresponding lineshape computed at the equilibrium configuration, using as an intrinsic width the value $\eta = 0.06E$ (dotted line). Although the intrinsic width adopted in [7] provides a larger smoothing which, due to its energy dependence, is more effective at high energies, the net result is similar to the one obtained with the coupling studied here, and we expect that besides Landau damping, which provides the dominant broadening mechanism, the

coupling to the normal modes accounts for most of the remaining effect [25].

Assuming that the intrinsic width is all due to the coupling mechanism studied here, we plot in Fig. 10 the strength functions of the two fullerenes, including this coupling, assuming a vibrational temperature of $T = 300$ K. In order to directly compare the two curves, we have plotted the strength per valence electron for both C_{60} and C_{70}. It is noteworthy the similarity of the two curves, the one associated with C_{70} being smoother than the one associated with C_{60}, in good agreement with the experimental results of [3]. In particular, the present coupling will be able to wash out the peak structure obtained for C_{70} in the visible-ultraviolet part of the absorption spectrum, at equilibrium configuration (Fig. 7).

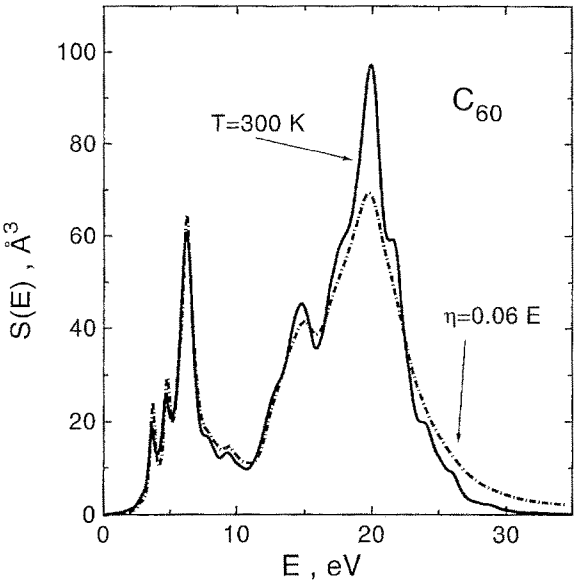

Fig. 9. Strength function of C_{60}: with a *solid line* is shown the resulting lineshape after the coupling considered here has been carried out at $T = 300$ K. The *dotted line* corresponds to the curve obtained by computing the response at equilibrium making use of an intrinsic width $\eta = 0.06E$

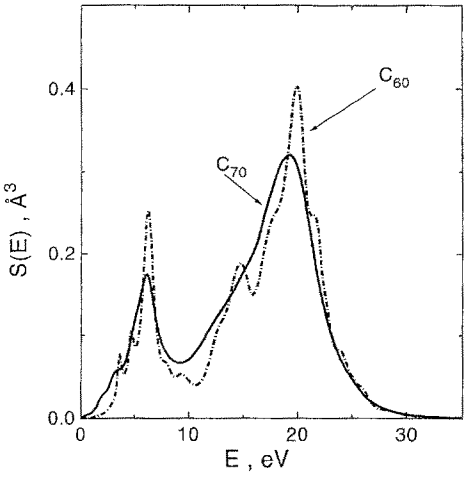

Fig. 10. Strength per valence electron for C_{60} (*dotted line*) and C_{70} (*solid line*). These results were obtained making use of the TB-LR, carrying out the coupling to the normal modes at $T = 300$ K

4 Conclusions

Making use of TB-LR formulation, we find that the lineshape and linewidth of the optical absorption spectra of C_{60} and C_{70} are dominated by Landau damping. In particular, Landau damping is large enough to wash out the deformation splitting effect associated with the anisotropy of the optical response of C_{70}.

By coupling the plasmon, excited on C_{60} and C_{70}, to the normal modes of vibration of these fullerenes, a sizeable contribution to its lineshape was obtained, consisting mostly of an effective and sizeable smoothing of the lineshape, without any significant change in the linewidth. The coupling was found to be effective already at $T = 0$, exhibiting a weak temperature dependence, C_{70} being somewhat more sensitive to the vibrational temperature than C_{60}.

Recently one has been able to synthesise large clusters, with several hundreds of carbon atoms, and which display elongated forms (carbon tubules). It is an easy task to show that, for these systems, there may be sizes for which deformation splitting will overcome Landau damping (contrary to C_{70}), leading eventually to a novel and interesting optical absorption structure. The deformation splitting may be able to "move" strength upwards in excitation energy, leading to an enhancement of the "bulk plasmon" [26] in these systems. That the interplay of these different microscopic mechanisms can be realized experimentally, remains a challenge for the future.

Discussions with B. Mottelson, D. Tomanek, R. Broglia, G. Bertsch and G. Benedek are gratefully acknowleged. One of us (JMP) would like to thank Carlos Jorge A.R. Pacheco for his help in producing the figures. This work has been partially supported by JNICT through the project PBICT/FIS/1635/93.

References

1. Ajie, H., Alvarez, M.M., Anz, S.J., Beck, R.D., Diederich, F., Fostiropoulos, K., Huffman, D.R., Krätschmer, W., Rubin, Y., Schriver, K.E., Sensharma, D., Whetten, R.L.: J. Phys. Chem. **94**, 8630 (1990)
2. Bertsch, G.F., Bulgac, A., Tomanek, D., Wang, Y.: Phys. Rev. Lett. **67**, 2690 (1991)
3. Hertel, I.V., Steger, H., de Vries, J., Weisser, B., Menzel, C., Kamke, B., Kamke, W.: Phys. Rev. Lett. **68**, 784 (1992)
4. Bulgac, A., Ju, N.: Phys. Rev. **B46**, 4297 (1992)
5. Keller, J.W., Coplan, M.A.: Chem. Phys. Lett. **193**, 89 (1992)
6. Ju, N., Bulgac, A., Keller, J.W.: Phys. Rev. **B48**, 9071 (1993)
7. Alasia, F., Roman, H.E., Broglia, R.A., Serra, Ll., Colò, G., Pacheco, J.M.: J. Phys. **B27**, L643 (1994)
8. We would like to point out that the high energy tail of the TDLDA response is artificially too high, constituting a finite basis-set effect. Indeed, the TDLDA calculations were performed in a spherical box, taking as a one-electron basis all eigenstates with an energy below 40 eV. This, being sufficient to describe the plasmon energy region, leads to a less accurate description at higher energies (for details, [7])
9. Pacheco, J.M., Broglia, R.A.: Phys. Rev. Lett. **62**, 1400 (1989)

10. Bertsch, G.F., Bortignon, P.F., Broglia, R.A.: Rev. Mod. Phys. **55**, 287 (1983)
11. Bortignon, P.F., Broglia, R.A., Bertsch, G.F., Pacheco, J.M.: Nucl. Phys. A**460**, 149 (1986)
12. Pacheco, J.M., Broglia, R.A., Mottelson, B.R.: Z. Phys. D**21**, 289 (1991)
13. Yannouleas, C., Pacheco, J.M., Broglia, R.A.: Phys. Rev. B**41**, 6088 (1990)
14. We are assuming that experiments are performed, as usual, with unpolarized cluster beams
15. Landau, L.D., Lifshitz, E.M.: Statistical physics, p. 89. Pergamon 1959
16. The adiabatic coupling written in (6) and (7) implicitly assumes that the potential energy surface associated with the photo-excited state does not change with respect to the one associated with the unexcited state. We expect this approximation to have small effects on the final results
17. Lepage, G.P.: J. Comput. Phys. **27**, 192 (1978)
18. Press, W.H., Farrar, G.R.: Comput. Phys. **4**, 190 (1990)
19. Benedek, G. et al.: Nuovo Cimento **15D**, 565 (1993)
20. While the value for η is immaterial (as long as it is small) for the calculation of the curves displayed in Figs. 4 and 5, it constitutes a compromise value in order to efficiently carry out the Monte-Carlo integrations. This value of η, ensures that an energy mesh of 0.1 eV will be enough to include all peaks in the absorption profile, with 350 underlying mesh points in each response calculation
21. Alasia, F., Roman, H.E., Broglia, R.A., Serra, Ll., Colò, G., Pacheco, J.M.: (in preparation). Preliminary results indicate, in fact, that the TB-LR results obtained here perform equally well in both C_{60} and C_{70}, when compared to ab initio TDLDA calculations. In particular, the anisotropy of response along the different axes in C_{70} is well reproduced by the present results
22. Onida, G., Benedek, G.: Europhys. Lett. **18**, 403 (1992)
23. Kohanoff, J., Andreoni, W., Parrinello, M.: Phys. Rev. B**46**, 4371 (1992)
24. Onida, G., Andreoni, W., Kohanoff, J., Parrinello, M.: Chem. Phys. Lett. **219**, 1 (1994)
25. In view of the results of [12], the study of this coupling beyond the adiabatic approximation would possibly result in a more asymmetric lineshape, with a more extended high energy tail
26. Bursill, L.A., Stadelmann, P.A., Peng, J.L., Prawer, S.: Phys. Rev. B**49**, 2882 (1994)